Available online at www.sciencedirect.com
ScienceDirect
Bioorganic & Medicinal Chemistry 16 (2008) 164–170
Bioorganic & Medicinal Chemistry

Characterization of distamycin A binding to damaged DNA

Aki Inase-Hashimoto,[a] Shinya Yoshikawa,[a] Yusuke Kawasaki,[a] Takashi S. Kodama[b] and Shigenori Iwai[a,*]

[a]*Division of Chemistry, Graduate School of Engineering Science, Osaka University, 1-3 Machikaneyama, Toyonaka, Osaka 560-8531, Japan*
[b]*Department of Medical Genetics, Osaka University Medical School, 2-2 Yamadaoka, Suita, Osaka 565-0871, Japan*

Received 28 August 2007; revised 19 September 2007; accepted 2 October 2007
Available online 5 October 2007

Abstract—We previously reported that distamycin A, a natural antibiotic known as a minor groove binder, could bind to DNA duplexes containing the (6–4) photoproduct formed at its target site, whereas the binding was not observed for duplexes containing the *cis-syn* cyclobutane pyrimidine dimer in the same sequence context. In this study, we have further analyzed the binding of this drug to lesion-containing duplexes to elucidate its damaged-DNA recognition mechanism. Surface plasmon resonance measurements using various types of DNA showed that distamycin A could bind to several types of lesion-containing DNA. Curve fitting of the CD titration data revealed that the complex formation occurred with K_d values around 10^{-6} and a stoichiometry of 1:1. The results obtained in this study suggested that distamycin A binds to damaged DNA in the same way as to the normal target site, by recognizing the chemical structure of the minor groove.

1. Introduction

Since DNA is an organic molecule, it is subjected to chemical reactions with both endogenous and exogenous substances in living organisms. The products, that is, DNA lesions, induce genetic mutations, which result in carcinogenesis and cell death. One of the important DNA-damaging factors is ultraviolet (UV) light in solar radiation.[1] UV light mainly causes two types of DNA lesions, the *cis–syn* cyclobutane pyrimidine dimer (CPD, Fig. 1a) and the pyrimidine(6–4)pyrimidone photoproduct ((6–4) photoproduct, Fig. 1b), which are formed at pyrimidine–pyrimidine sequences. Among these lesions, the CPD is repaired more slowly in cells,[2,3] but the DNA containing this lesion can be replicated correctly by a DNA polymerase responsible for translesion synthesis.[4–6] Although the (6–4) photoproduct is more mutagenic than the CPD,[7–9] this photoproduct is a good substrate for nucleotide excision repair (NER)[10,11] and thus is efficiently repaired in cells.[2,3] In human cells, the UV-damaged DNA-binding (UV-DDB) protein, which is inactivated by mutation in xeroderma pigmentosum (XP) group E cells, has high affinity for DNA containing the (6–4) photoproduct.[12,13] Upon its binding to damaged DNA, the associated ubiquitin ligase ubiquitylates both the UV-DDB and XP group C (XPC) proteins, and this ubiquitylation transfers the damaged DNA from the UV-DDB protein to the XPC-HR23B complex,[14] which initiates global-genome NER.[15] Defects in NER cause hereditary diseases, such as XP, Cockayne syndrome, and trichothiodystrophy.[16,17]

In our previous study, we found that distamycin A (Fig. 1c), a natural antibiotic known as a minor groove binder, could bind to DNA containing a (6–4) photoproduct formed at its AATT target site, although the binding was not observed for duplexes containing a CPD in the same sequence context.[18] In the (6–4) photoproduct, the chemical structure of the 3′ pyrimidone base is quite different from that of the original pyrimidine base, and the two base rings are perpendicular to each other, whereas CPD formation causes only small changes in both the chemical and tertiary structures.[19] Therefore, the above results suggested that the recognition mechanism of distamycin A for the (6–4) photoproduct-containing DNA would differ from that for the natural A·T-rich target site. Recently, we found that

Keywords: DNA damage; Drug–DNA interactions; Surface plasmon resonance; Circular dichroism.
* Corresponding author. Tel.: +81 6 6850 6250; fax: +81 6 6850 6240; e-mail: iwai@chem.es.osaka-u.ac.jp

0968-0896/$ - see front matter © 2007 Elsevier Ltd. All rights reserved.
doi:10.1016/j.bmc.2007.10.002

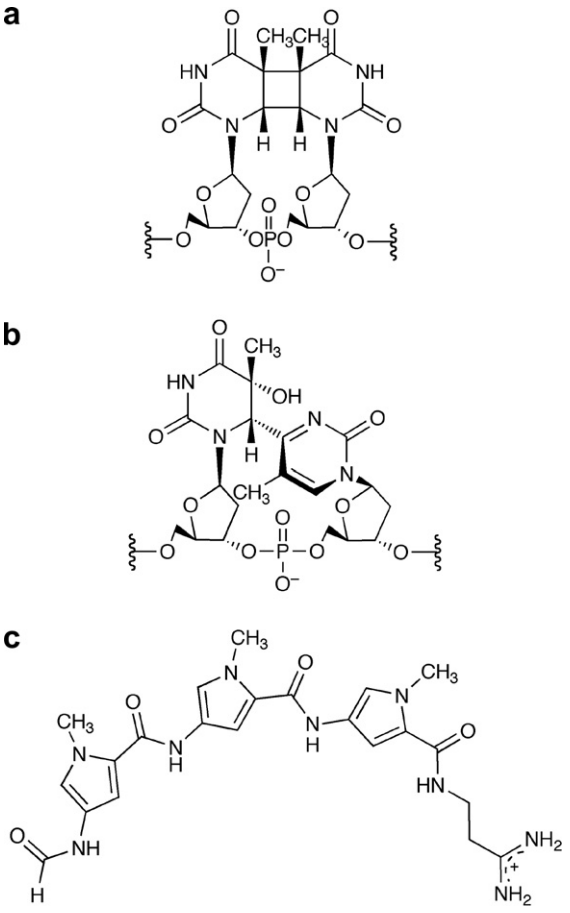

Figure 1. Chemical structures of the CPD (a), the (6–4) photoproduct (b), and distamycin A (c).

distamycin A could bind to DNA containing thymine glycol, an oxidative DNA lesion, regardless of the opposite base.[20] When distamycin A binds to the AAT-T·AATT sequence, a single molecule of this compound fits snugly into the minor groove, and the amide protons of the drug form hydrogen bonds with the N3 of adenine and the O2 of thymine.[21–23] However, there is no structural information available on its binding to duplexes containing lesions that cause changes in both the chemical and local tertiary structures. Understanding the mechanism by which distamycin A interacts with damaged DNA will provide insight into a new function of this drug, which may lead to its use in an artificial repair system for this type of UV damage. In this study, the drug binding to duplexes containing other types of base lesions was determined by surface plasmon resonance (SPR) measurements and by circular dichroism (CD) spectroscopy. Based on the results, the structure–function relationship of the binding site for distamycin A is discussed.

2. Results

2.1. Distamycin A binding to various types of lesions

The binding of distamycin A to damaged DNA was originally found for the (6–4) photoproduct, in contrast to the negative result for the CPD in the same sequence context,[18] and subsequently was found for thymine glycol.[20] To define the factors in the lesion-containing duplexes that are recognized by distamycin A, we examined the drug binding to duplexes containing other types of lesions. Although the drug binding was analyzed by CD titration experiments in the original report,[18] the present screening-type study was performed by SPR measurements, which yielded distinctive results in our recent work.[20] Nonspecific binding could be suppressed by using low drug concentrations. Duplexes, d(CCT ACGCGAA-X_1X_2-CGGCATCC)·biotin-d(GGATGC CG-Y_2Y_1-TTCGCGTAGG), with the combinations of X_1, X_2, Y_1, and Y_2 shown in Table 1, were prepared and immobilized on streptavidin-linked sensor chips. In our previous study,[18] 14-bp duplexes were used for the CD experiments, but we found that 14-bp duplexes containing a lesion, such as a synthetic analog of the apurinic/apyrimidinic (AP) site, were dissociated on the sensor chip during repeated measurements. Therefore, relatively long 20-bp duplexes were chosen in this study, and their integrity during the measurements was confirmed by dissociating the hybridized strand on the sensor chip with an HCl solution after the analysis. A different sequence was used for the cisplatin-adducted duplex, for preparation reasons. The designations of the duplexes are listed in Table 1, and the results are shown in Figures 2 and 3. AP·A-20, containing 1′,2′-dideoxyribose as an AP site analog, yielded sensorgrams indicating distamycin A binding (Fig. 2d), although the response was somewhat lower than that for T·A-20 (Fig. 2a), which was used as a positive control in this study. However, the binding was lost when the opposite base was changed from adenine to cytosine (Fig. 2e) or to guanine (data not shown). The other lesions we tested in this study included the cisplatin adduct, 7,8-dihydro-8-oxoguanine (OG), O^6-methylguanine (MG), a mismatch, and a 2-bp mismatch. Among them, the MG-containing duplex (MG·C-20) generated binding sensorgrams, as shown in Figure 2g, although the increase was relatively small. It should be noted that distamycin A could not bind to a G·C pair-containing target site, AAGT·ACTT, as shown in Figure 2b.

In order to determine the reason for the unexpected binding of distamycin A to MG·C-20, the drug binding was analyzed with a few more duplexes. Since O^6-alkylguanine forms a wobble pair with cytosine,[24–26] duplexes containing Watson–Crick (MG·T-20), wobble (G·T-20), and *syn–anti* (OG·A-20 and G·A-20) base pairs were prepared. As shown in Figure 3, OG·A-20 and G·A-20 exhibited specific binding, and the increase in response units observed for OG·A-20 was larger than that for T·A-20.

2.2. Analysis of the distamycin A binding by CD spectroscopy

The results of the SPR measurements revealed that distamycin A could bind to several types of lesion-containing duplexes. The binding to these duplexes was analyzed in detail by CD spectroscopy. Using T·A-20, AP·A-20, MG·C-20, OG·A-20, and G·A-20, without

Table 1. Oligonucleotide duplexes used for the SPR analysis[a]

Designation	X_1	X_2	Y_1	Y_2
T·A-20	T	T	A	A
G·C-20	G	T	C	A
CP-20[b]	Cisplatin adduct of GG		C	C
AP·A-20	AP site analog	T	A	A
AP·C-20	AP site analog	T	C	A
OG·C-20	7,8-Dihydro-8-oxoguanine	T	C	A
MG·C-20	O^6-methylguanine	T	C	A
MM-20	T	T	C	A
2MM-20[b]	T	T	C	C
MG·T-20	O^6-methylguanine	T	T	A
G·T-20	G	T	T	A
OG·A-20	7,8-Dihydro-8-oxoguanine	T	A	A
G·A-20	G	T	A	A

[a] The DNA lesions were incorporated into the sequence 5′-CCTACGCGAA-X_1X_2-CGGCATCC-3′·3′-GGATGCGCTT-Y_1Y_2-GCCGTAGG-biotin-5′.

[b] The sequence was 5′-CCACCACCTT-X_1X_2-CCTCCTCC-3′·3′-GGTGGTGGAA-Y_1Y_2-GGAGGAGG-biotin-5′.

the biotin moiety for the attachment to the sensor chips in the SPR analysis, CD titration experiments were performed in the same way as in our previous study.[18] To reduce nonspecific binding, CD spectra were measured at 37 °C. Duplex formation at this temperature was confirmed by measuring the melting curve of each duplex (data not shown). As shown in Figure 4, induced CD signals, which indicated the specific binding of distamycin A, were observed at wavelengths between 300 and 360 nm. The spectral changes observed for AP·A-20, MG·C-20, OG·A-20, and G·A-20 were very similar to that for T·A-20. The ellipticity values at 325 nm were plotted against the distamycin/duplex ratios, as shown in Figure 5. The slopes for T·A-20 and OG·A-20 were steep, and reached a plateau within the tested range of drug concentrations. On the other hand, the slopes obtained for AP·A-20, MG·C-20, and G·A-20 were gentle, and the increase in the signal intensity persisted at the high drug concentrations in these cases. The distamycin A binding to each duplex was analyzed by curve fitting of the CD titration data. The dissociation constants (K_d) and the stoichiometries (n) that gave the best-fit curves shown in Figure 5 are summarized in Table 2. The affinity of distamycin A for OG·A-20 was similar to that for T·A-20, and the K_d values obtained for AP·A-20, MG·C-20, and G·A-20 were somewhat larger than that for T·A-20, as predicted from the SPR experiments. Since a single distamycin A molecule binds to duplexes containing the AATT·AATT site, like T·A-20,[21–23] the calculated n values indicate that similar 1:1 binding occurs with the other duplexes listed in Table 2.

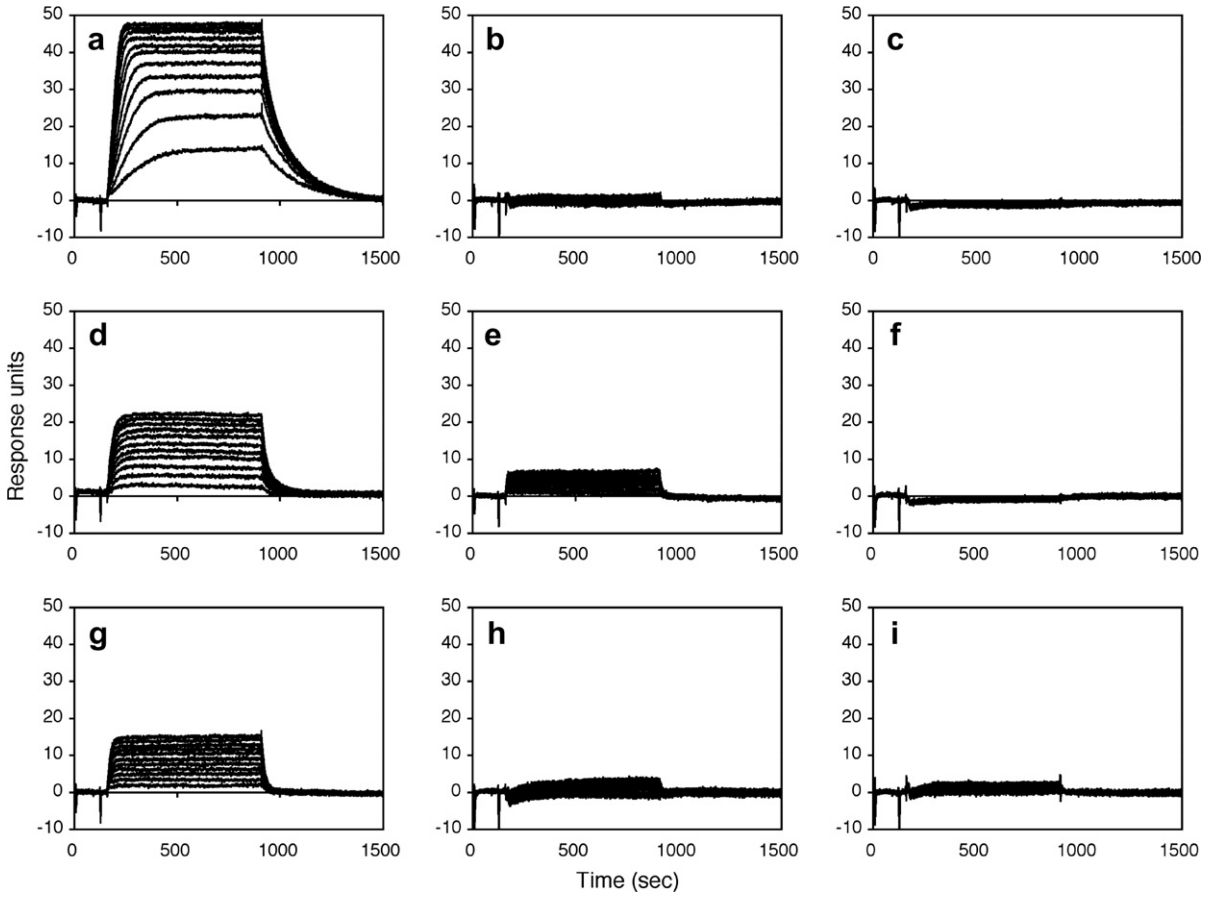

Figure 2. SPR analysis of the distamycin A binding to T·A-20 (a), G·C-20 (b), CP-20 (c), AP·A-20 (d), AP·C-20 (e), OG·C-20 (f), MG·C-20 (g), MM-20 (h), and 2MM-20 (i). The concentrations of distamycin A were 5, 10, 15, 20, 25, 30, 35, 40, 45, 50, and 55 nM.

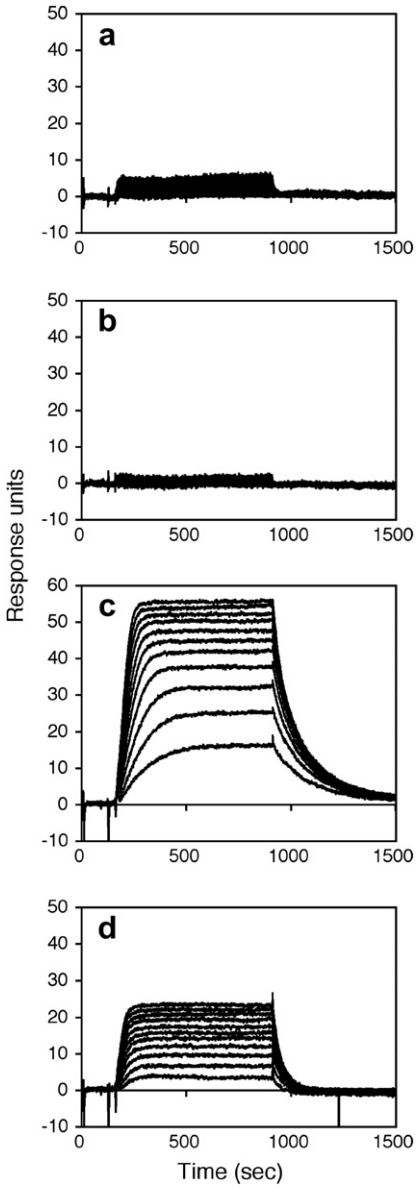

Figure 3. SPR analysis of the distamycin A binding to MG·T-20 (a), G·T-20 (b), OG·A-20 (c), and G·A-20 (d). The concentrations of distamycin A were 5, 10, 15, 20, 25, 30, 35, 40, 45, 50, and 55 nM.

3. Discussion

Distamycin A is a well-characterized minor groove binder, and its DNA recognition mechanism has been elucidated at atomic resolution.[21–23,27–31] The target sites are stretches of A·T-rich sequences, but we found that this drug bound to duplexes containing the (6–4) photoproduct in its minimum target site, AATT·AATT, whereas CPD formation at this site prevented the drug binding.[18] Both of these lesions are formed by a [2 + 2] photocycloaddition as a result of excitation of the double bonds in adjacent pyrimidines by UV irradiation, but the former one has chemical and tertiary structures that are completely altered from those of the original pyrimidine base.[19,32–34] These alterations lead to higher mutation frequencies in cells.[7–9] Although the (6–4) photoproduct is efficiently repaired by NER,[10,11] there is a hereditary disease, XP, caused by the lack of this repair pathway.[17] If we can develop a molecule that recognizes the (6–4) photoproduct and degrades it at least partially, this UV lesion may become a substrate for the base excision repair, which is another pathway intact in the XP patients, and such a molecule is a candidate for a preventive for skin cancer. Toward this aim, we have analyzed the binding of distamycin A to damaged DNA.

In order to determine the factors recognized by distamycin A, its binding to various lesion-containing duplexes was analyzed in this study. The initial screening was carried out by the SPR measurements (Figs. 2 and 3), and quantitative analysis of the distamycin A binding to the screened duplexes was performed by CD spectroscopy (Figs. 4 and 5). Although the conditions were considerably different between the SPR and CD experiments, there was a good correlation between the results. The order of the affinity of distamycin A calculated from the CD titration data was OG·A-20 $\geqslant$ T·A-20 > AP·A-20 $\geqslant$ G·A-20 > MG·C-20, which agreed with that of the increase in the SPR response.

In the SPR experiments, AP·A-20, which contained an AP site analog opposite adenine, yielded sensorgrams showing specific binding of distamycin A (Fig. 2d), but the affinity was greatly reduced when the unpaired base was changed to cytosine (Fig. 2e). This result suggested that distamycin A recognized the imperfect target sequence, AA–T·AATT, but not the AP site itself or the nature of the AP-containing duplex. The reduced affinity for AP·A-20, as compared to T·A-20, can be attributed to this recognition mode. The duplex containing an MG·C pair bound distamycin A (Fig. 2g), whereas those containing an MG·T pair and a G·T mismatch did not yield binding sensorgrams (Fig. 3a and b, respectively). In the case of OG, the effect of the opposite base was different. While distamycin A did not bind to a duplex containing the OG·C pair (Fig. 2f), obvious binding was observed when the opposite base was changed to adenine (Fig. 3c). The same results were obtained for G·C-20 and G·A-20 (Figs. 2b and 3d, respectively).

Since the duplexes to which distamycin A bound in this study were modified at a single site within the AAT-T·AATT target sequence, we considered the chemical structures of the base pairs at this site. As shown in Figure 6, a Watson–Crick-type base pair is formed between MG and thymine,[35,36] but when MG is opposite cytosine, the positions of the two bases are slightly shifted to form a wobble pair, with hydrogen bonds between the N1 of MG and the NH_2 of C, and between the NH_2 of MG and the N3 of C.[24–26] Another type of wobble pair is formed between guanine and thymine.[37,38] Distamycin A binds to a duplex containing a T·A pair at this site (Fig. 2a), but not to that containing a G·C pair (Fig. 2b). The difference is that there is steric hindrance (the amino function of guanine) in the minor groove in the latter case, as shown in Figure 6, and the amide protons of the distamycin A molecule form hydrogen bonds with the O2 of thymine and the N3 of adenine at the 4-bp target site.[22,23] Among the three structures of MG·T, MG·C, and G·T in Figure 6, only the MG·C pair meets

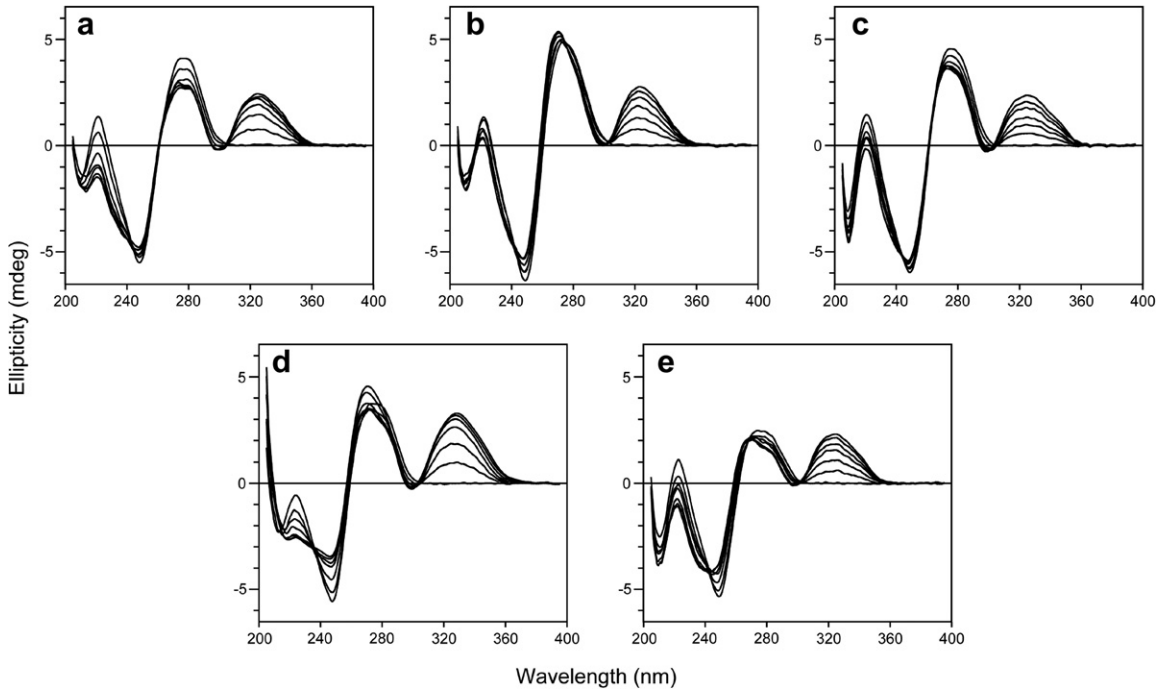

Figure 4. CD spectra showing the distamycin A binding to T·A-20 (a), AP·A-20 (b), MG·C-20 (c), OG·A-20 (d), and G·A-20 (e). The drug/DNA ratios were 0, 0.5, 1.0, 1.5, 2.0, 2.5, and 3.0.

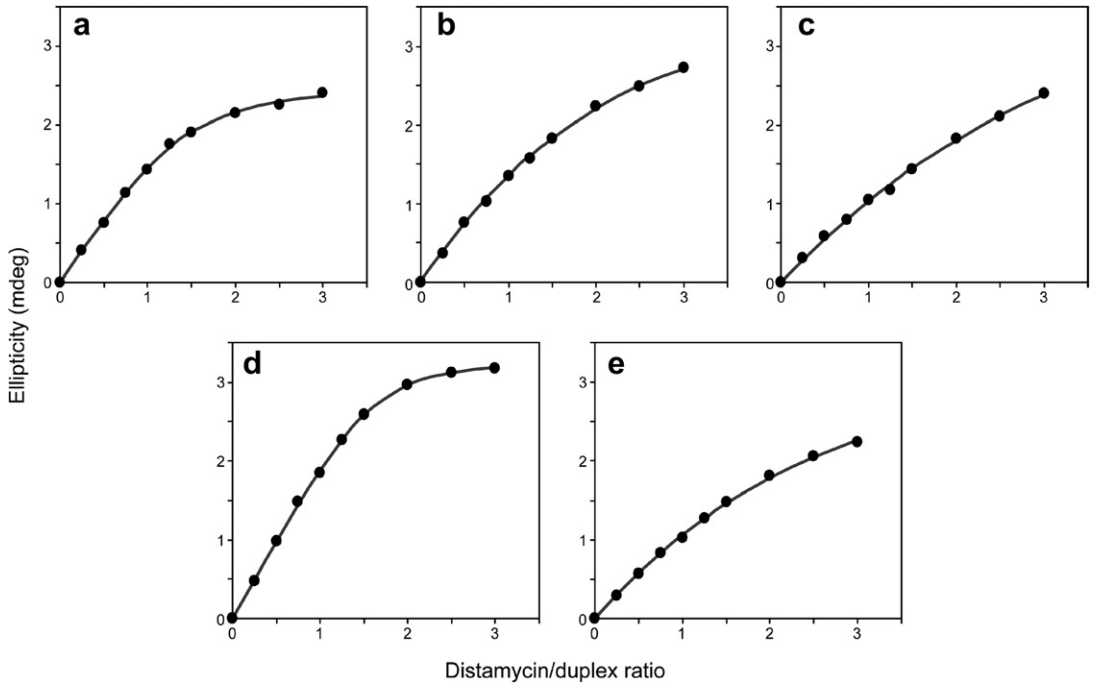

Figure 5. CD titration plots and best-fit curves for the distamycin A binding to T·A-20 (a), AP·A-20 (b), MG·C-20 (c), OG·A-20 (d), and G·A-20 (e).

Table 2. Binding parameters obtained from the CD titration curves

Duplex	K_d (M)	n (per duplex)
T·A-20	3.7×10^{-7}	1.43
AP·A-20	2.0×10^{-6}	1.71
MG·C-20	7.6×10^{-6}	1.70
OG·A-20	2.0×10^{-7}	1.61
G·A-20	3.7×10^{-6}	1.66

the requirements for distamycin A binding; namely, a less-hindered minor groove with two hydrogen-bond acceptors. This also applies to the OG·A pair and the G·A mismatch (Fig. 5c and d, respectively). In the former case, OG adopts a *syn* conformation and forms hydrogen bonds with adenine, as shown in Figure 6,[39,40] and because the structure of the minor groove side of this base pair is very similar to that of the T·A pair, it is reasonable that dista-

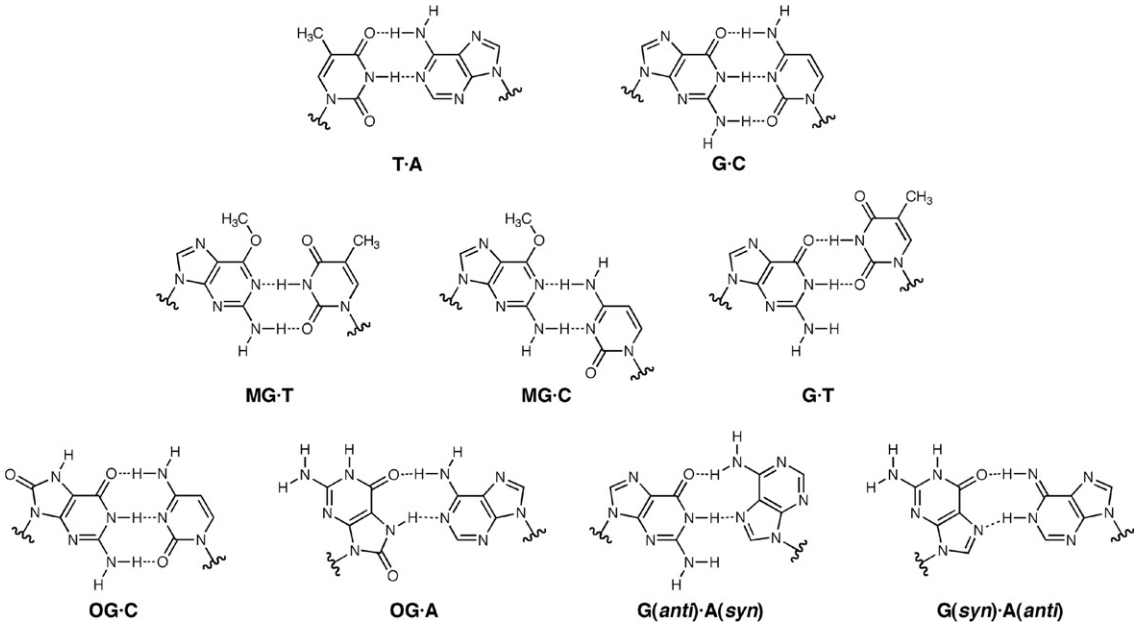

Figure 6. Structures of the base pairs discussed in this study.

mycin A can bind to OG·A-20 with high affinity. In the latter case, two types of unusual base pairs, G(*anti*)·A(*syn*)[41,42] and G(*syn*)·A(*anti*),[43] have been reported. The observed binding of distamycin A to G·A-20, with a lower affinity, suggests the formation of the G(*syn*)·A(*anti*) pair, which only lacks the 8-oxo function in the OG·A pair. As discussed here, the distamycin A binding that was observed for the duplexes containing a monomeric lesion used in this study can be explained by the chemical structure of the minor groove side of the base pair.

How can we correlate these results to the recognition of dimeric UV lesions by distamycin A? As shown in Figure 1b, the chemical structure of the 3′ component of the (6–4) photoproduct is greatly altered from that of the original pyrimidine base, and this moiety is linked perpendicularly to the 5′ component.[32,33] However, it may be possible that the O2 atom of the 3′ pyrimidone, which is thrust into the minor groove,[34] is accidentally located at the same position as the O2 of the thymine base in the T·A base pair and acts as a hydrogen-bond acceptor in the complex formation with distamycin A. By CD spectroscopy, we confirmed that this drug did not bind to a duplex containing the Dewar valence isomer of the (6–4) photoproduct, in which the chemical structure of the 3′ component was altered (data not shown), which supports the above idea. In the CPD, the functional groups are not changed from those of the original thymine bases, as shown in Figure 1a, but their spatial arrangement is slightly altered by the CPD formation,[44] because the C5 and C6 atoms in the CPD have sp^3 hybrid orbitals with tetrahedral bond angles. This alteration should affect the binding of distamycin A.

In this study, we have shown that distamycin A can bind to several types of damaged DNA in the 1:1 binding mode. We propose that the recognition of lesion-containing duplexes by this drug depends on the chemical structure of the minor groove side of the base pair. Distamycin A may recognize the (6–4) photoproduct-containing duplex in the same manner.

4. Experimental

4.1. Materials

Oligonucleotides were synthesized on an Applied Biosystems Model 3400 DNA synthesizer (Applied Biosystems, Foster City, CA). The biotin moiety at the 5′ end of the oligonucleotides for the SPR measurements was attached using 5′-biotin phosphoramidite [[1-*N*-(4,4′-dimethoxytrityl)-biotinyl-6-aminohexyl]-(2-cyanoethyl)-*N*,*N*-diisopropylphosphoramidite] from Glen Research (Sterling, VA). Oligonucleotides containing the AP site analog, OG, and MG were synthesized using the corresponding phosphoramidites (Glen Research). The cisplatin adduct was formed by treating a 20-mer, d(CCACCACCTTGGCCTCCTCC), with 1.2 equiv of *cis*-diamminedichloroplatinum(II) (EMD Biosciences, La Jolla, CA) in water at room temperature for 3 days. These oligonucleotides were purified by HPLC, using a μBondasphere C18 5 μm 300 Å column (3.9 × 150 mm, Waters Corporation, Milford, MA) or a μBondasphere C18 15 μm 300 Å column (7.8 × 300 mm) with a linear gradient of acetonitrile in 0.1 M triethylammonium acetate (pH 7.0). Duplexes were formed by heating aqueous solutions of the two strands to 80 °C for 3 min and cooling them gradually to room temperature. Distamycin A hydrochloride was purchased from Serva Electrophoresis (Heidelberg, Germany).

4.2. SPR measurements

Experiments were performed on a Biacore 2000 system, using streptavidin sensor chips (Biacore Sensor Chip

SA). The duplexes were immobilized at a flow rate of 5 μL/min with a DNA concentration of 100 nM, using a buffer containing 10 mM sodium phosphate (pH 7.0), 500 mM NaCl, 3 mM EDTA, and 0.005% Tween 20, and the amount of the immobilized duplex was about 900 resonance units. One flow cell was left intact and was used as a blank for reference. The sensorgrams were collected at a flow rate of 20 μL/min, using the same buffer. All of the experiments were performed at 15 °C, to avoid dissociation of the duplexes.

4.3. CD spectroscopy

The CD spectra of the distamycin A–20 bp DNA complexes were measured at 37 °C, in a buffer containing 10 mM sodium phosphate (pH 7.0) and 500 mM NaCl, on a JASCO J-805 spectrophotometer. The sample solutions (600 μL) contained 2.5 μM of each duplex listed in Table 2, and the titration was conducted by adding 1.5 μL or 0.75 μL of 0.5 mM distamycin A to increase the drug/duplex molar ratio by 0.5 or 0.25, respectively. The titration data obtained at 325 nm in the CD spectra were analyzed by the nonlinear least-squares fitting method, as described previously.[18]

Acknowledgments

This study was supported by a Grant-in-Aid for Scientific Research from the Ministry of Education, Culture, Sports, Science and Technology, Japan. A.I.H. was supported by a Research Fellowship of the Japan Society for the Promotion of Science for Young Scientists.

References and notes

1. Cadet, J.; Courdavault, S.; Ravanat, J.-L.; Douki, T. *Pure Appl. Chem.* **2005**, *77*, 947.
2. Perdiz, D.; Gróf, P.; Mezzina, M.; Nikaido, O.; Moustacchi, E.; Sage, E. *J. Biol. Chem.* **2000**, *275*, 26732.
3. Courdavault, S.; Baudouin, C.; Charveron, M.; Canguilhem, B.; Favier, A.; Cadet, J.; Douki, T. *DNA Repair* **2005**, *4*, 836.
4. Masutani, C.; Araki, M.; Yamada, A.; Kusumoto, R.; Nogimori, T.; Maekawa, T.; Iwai, S.; Hanaoka, F. *EMBO J.* **1999**, *18*, 3491.
5. Masutani, C.; Kusumoto, R.; Yamada, A.; Dohmae, N.; Yokoi, M.; Yuasa, M.; Araki, M.; Iwai, S.; Takio, K.; Hanaoka, F. *Nature* **1999**, *399*, 700.
6. Masutani, C.; Kusumoto, R.; Iwai, S.; Hanaoka, F. *EMBO J.* **2000**, *19*, 3100.
7. LeClerc, J. E.; Borden, A.; Lawrence, C. W. *Proc. Natl. Acad. Sci. U.S.A.* **1991**, *88*, 9685.
8. Smith, C. A.; Wang, M.; Jiang, N.; Che, L.; Zhao, X.; Taylor, J.-S. *Biochemistry* **1996**, *35*, 4146.
9. Kamiya, H.; Iwai, S.; Kasai, H. *Nucleic Acids Res.* **1998**, *26*, 2611.
10. Svoboda, D. L.; Smith, C. A.; Taylor, J.-S.; Sancar, A. *J. Biol. Chem.* **1993**, *268*, 10694.
11. Sugasawa, K.; Okamoto, T.; Shimizu, Y.; Masutani, C.; Iwai, S.; Hanaoka, F. *Genes Dev.* **2001**, *15*, 507.
12. Reardon, J. T.; Nichols, A. F.; Keeney, S.; Smith, C. A.; Taylor, J.-S.; Linn, S.; Sancar, A. *J. Biol. Chem.* **1993**, *268*, 21301.
13. Fujiwara, Y.; Masutani, C.; Mizukoshi, T.; Kondo, J.; Hanaoka, F.; Iwai, S. *J. Biol. Chem.* **1999**, *274*, 20027.
14. Sugasawa, K.; Okuda, Y.; Saijo, M.; Nishi, R.; Matsuda, N.; Chu, G.; Mori, T.; Iwai, S.; Tanaka, K.; Tanaka, K.; Hanaoka, F. *Cell* **2005**, *121*, 387.
15. Sugasawa, K.; Ng, J. M. Y.; Masutani, C.; Iwai, S.; van der Spek, P. J.; Eker, A. P. M.; Hanaoka, F.; Bootsma, D.; Hoeijmakers, J. H. J. *Mol. Cell* **1998**, *2*, 223.
16. Lehmann, A. R. *Biochimie* **2003**, *85*, 1101.
17. Cleaver, J. E. *Nat. Rev. Cancer* **2005**, *5*, 564.
18. Inase, A.; Kodama, T. S.; Sharif, J.; Xu, Y.; Ayame, H.; Sugiyama, H.; Iwai, S. *J. Am. Chem. Soc.* **2004**, *126*, 11017.
19. Kim, J.-K.; Patel, D.; Choi, B.-S. *Photochem. Photobiol.* **1995**, *62*, 44.
20. Shimizu, T.; Manabe, K.; Yoshikawa, S.; Kawasaki, Y.; Iwai, S. *Nucleic Acids Res.* **2006**, *34*, 313.
21. Klevit, R. E.; Wemmer, D. E.; Reid, B. R. *Biochemistry* **1986**, *25*, 3296.
22. Pelton, J. G.; Wemmer, D. E. *Biochemistry* **1988**, *27*, 8088.
23. Uytterhoeven, K.; Sponer, J.; Van Meervelt, L. *Eur. J. Biochem.* **2002**, *269*, 2868.
24. Patel, D. J.; Shapiro, L.; Kozlowski, S. A.; Gaffney, B. L.; Jones, R. A. *Biochemistry* **1986**, *25*, 1027.
25. Kalnik, M. W.; Li, B. F. L.; Swann, P. F.; Patel, D. J. *Biochemistry* **1989**, *28*, 6182.
26. Sriram, M.; van der Marel, G. A.; Roelen, H. L. P. F.; van Boom, J. H.; Wang, A. H.-J. *EMBO J.* **1992**, *11*, 225.
27. Pelton, J. G.; Wemmer, D. E. *Proc. Natl. Acad. Sci. U.S.A.* **1989**, *86*, 5723.
28. Pelton, J. G.; Wemmer, D. E. *J. Am. Chem. Soc.* **1990**, *112*, 1393.
29. Coll, M.; Frederick, C. A.; Wang, A. H.-J.; Rich, A. *Proc. Natl. Acad. Sci. U.S.A.* **1987**, *84*, 8385.
30. Chen, X.; Ramakrishnan, B.; Rao, S. T.; Sundaralingam, M. *Struct. Biol.* **1994**, *1*, 169.
31. Chen, X.; Ramakrishnan, B.; Sundaralingam, M. *J. Mol. Biol.* **1997**, *267*, 1157.
32. Rycyna, R. E.; Alderfer, J. L. *Nucleic Acids Res.* **1985**, *13*, 5949.
33. Taylor, J.-S.; Garrett, D. S.; Wang, M. J. *Biopolymers* **1988**, *27*, 1571.
34. Kim, J.-K.; Choi, B.-S. *Eur. J. Biochem.* **1995**, *228*, 849.
35. Leonard, G. A.; Thomson, J.; Watson, W. P.; Brown, T. *Proc. Natl. Acad. Sci. U.S.A.* **1990**, *87*, 9573.
36. Vojtechovsky, J.; Eaton, M. D.; Gaffney, B.; Jones, R.; Berman, H. M. *Biochemistry* **1995**, *34*, 16632.
37. Hunter, W. N.; Brown, T.; Kneale, G.; Anand, N. N.; Rabinovich, D.; Kennard, O. *J. Biol. Chem.* **1987**, *262*, 9962.
38. Allawi, H. T.; SantaLucia, J., Jr. *Nucleic Acids Res.* **1998**, *26*, 4925.
39. Kouchakdjian, M.; Bodepudi, V.; Shibutani, S.; Eisenberg, M.; Johnson, F.; Grollman, A. P.; Patel, D. J. *Biochemistry* **1991**, *30*, 1403.
40. McAuley-Hecht, K. E.; Leonard, G. A.; Gibson, N. J.; Thomson, J. B.; Watson, W. P.; Hunter, W. N.; Brown, T. *Biochemistry* **1994**, *33*, 10266.
41. Brown, T.; Hunter, W. N.; Kneale, G.; Kennard, O. *Proc. Natl. Acad. Sci. U.S.A.* **1986**, *83*, 2402.
42. Webster, G. D.; Sanderson, M. R.; Skelly, J. V.; Neidle, S.; Swann, P. F.; Li, B. F.; Tickle, I. J. *Proc. Natl. Acad. Sci. U.S.A.* **1990**, *87*, 6693.
43. Leonard, G. A.; Booth, E. D.; Brown, T. *Nucleic Acids Res.* **1990**, *18*, 5617.
44. McAteer, K.; Jing, Y.; Kao, J.; Taylor, J.-S.; Kennedy, M. A. *J. Mol. Biol.* **1998**, *282*, 1013.